THE JOURNAL OF BIOLOGICAL CHEMISTRY VOL. 283, NO. 29, pp. 20060–20068, July 18, 2008

Histone Arg Modifications and p53 Regulate the Expression of *OKL38*, a Mediator of Apoptosis*[S]

Received for publication, April 17, 2008, and in revised form, May 21, 2008 Published, JBC Papers in Press, May 22, 2008, DOI 10.1074/jbc.M802940200

Hongjie Yao[‡], Pingxin Li[‡], Bryan J. Venters[‡], Suting Zheng[‡], Paul R. Thompson[§], B. Franklin Pugh[‡], and Yanming Wang[‡1]

From the [‡]Center for Gene Regulation, Department of Biochemistry and Molecular Biology, Pennsylvania State University, University Park, Pennsylvania 16802 and the [§]Department of Chemistry and Biochemistry, University of South Carolina, Columbia, South Carolina 29208

Protein Arg methyltransferases function as coactivators of the tumor suppressor p53 to regulate gene expression. Peptidylarginine deiminase 4 (PAD4/PADI4) counteracts the functions of protein Arg methyltransferases in gene regulation by deimination and demethylimination. Here we show that the expression of a tumor suppressor gene, *OKL38*, is activated by the inhibition of PAD4 or the activation of p53 following DNA damage. Chromatin immunoprecipitation assays showed a dynamic change of p53 and PAD4 occupancy and histone Arg modifications at the *OKL38* promoter during DNA damage, suggesting a direct role of PAD4 and p53 in the expression of OKL38. Furthermore, we found that OKL38 induces apoptosis through localization to mitochondria and induction of cytochrome *c* release. Together, our studies identify *OKL38* as a novel p53 target gene that is regulated by PAD4 and plays a role in apoptosis.

Post-translational histone modifications play pivotal roles in chromatin-templated nuclear events, such as transcription and DNA damage repair (1–3). Histone Arg methylation catalyzed by members of the protein Arg methyltransferase family correlates with transcriptional activation of β-globin, nuclear receptor, and p53 target genes (4–9). Peptidylarginine deiminases (PADs)[2] are a family of enzymes previously known to convert protein Arg residues to citrulline (Cit, a nonconventional amino acid in proteins) (10–12). In searching for enzymes that reverse histone Arg methylation, we and others (13–15) have identified peptidylarginine deiminase 4 (PAD4/PADI4). We showed that, in addition to deimination of Arg residues, PAD4 can convert monomethyl-Arg residues in histones to Cit and release methylamine in a previously uncharacterized reaction termed demethylimination (15). Several studies have found that PAD4 plays a repressive role in the expression of genes activated by estrogen and retinoic acid receptors (13, 15, 16). Our recent work has found that PAD4 interacts with p53 and represses the expression of p53 target gene *p21* (17).

p53 is at a pivotal center in regulating the cell cycle and apoptosis in response to various genotoxic stresses (18, 19). Upon activation, p53 turns on the expression of proapoptosis genes, including *BAX*, a Bcl-2 protein family member (20), *p53 AIP1* (21), and *NOXA* (22). These downstream target genes in turn execute apoptosis, an evolutionarily conserved cell death process characterized by DNA fragmentation, apoptotic body formation, and cytochrome *c* release (23, 24).

To further understand the role of PAD4 in gene regulation, we performed DNA microarray analysis to identify genes regulated by PAD4 activity in cells treated with Cl-amidine, a recently described PAD4 inhibitor (25). Here we report that the expression of a putative tumor suppressor gene, *OKL38/BDGI* (26, 27), was significantly induced by Cl-amidine treatment in several cancer cell lines. Bioinformatic and electrical mobility shift analyses identified a putative p53-binding site at the promoter of OKL38. Chromatin immunoprecipitation (ChIP) assays indicated that an increase in p53 binding and histone Arg methylation, as well as a decrease in PAD4 association and histone citrullination on the *OKL38* promoter, temporally correlates with the activation of OKL38 after DNA damage treatment. Although several studies suggested that the loss of OKL38 correlates with the tumorigenesis process, the mechanisms by which OKL38 induces cell death is unclear. We found that OKL38 induces cytochrome *c* release from mitochondria and that the localization of OKL38 to mitochondria correlates with its proapoptosis function.

EXPERIMENTAL PROCEDURES

Cell Culture and Cell Treatments with Cl-amidine, Doxycycline, Doxorubicin, and siRNAs—These procedures are described in detail in the supplemental material.

Plasmid Construction, Antibody Generation, Quantitative RT-PCR, and Chromatin Immunoprecipitation—Details about these procedures are described in the supplemental material.

Electrophoretic Mobility Shift Assay—Electrophoretic mobility shift assay (EMSA) was performed according to a method described previously (28), with some modifications. Oligonu-

* This work was supported, in whole or in part, by National Institutes of Health Grant GM079357 (to P. R. T.). This work was also supported by a startup fund from Pennsylvania State University (to Y. W.) and a TSF seed grant award from Johnson & Johnson Inc. and Pennsylvania State University. The costs of publication of this article were defrayed in part by the payment of page charges. This article must therefore be hereby marked "*advertisement*" in accordance with 18 U.S.C. Section 1734 solely to indicate this fact.

[S] The on-line version of this article (available at http://www.jbc.org) contains supplemental Experimental Procedures, additional references, and Figs. S1–S7.

[1] To whom correspondence should be addressed: 332 South Frear, University Park, PA 16802. E-mail: yuw12@psu.edu.

[2] The abbreviations used are: PAD, peptidylarginine deiminase; Cit, citrulline; qRT, quantitative reverse transcription; GAPDH, glyceraldehyde-3-phosphate dehydrogenase; siRNA, short interfering RNA; EMSA, electrophoretic mobility shift assay; ChIP, chromatin immunoprecipitation; NPM, nucleophosmin; oligo, oligonucleotide.

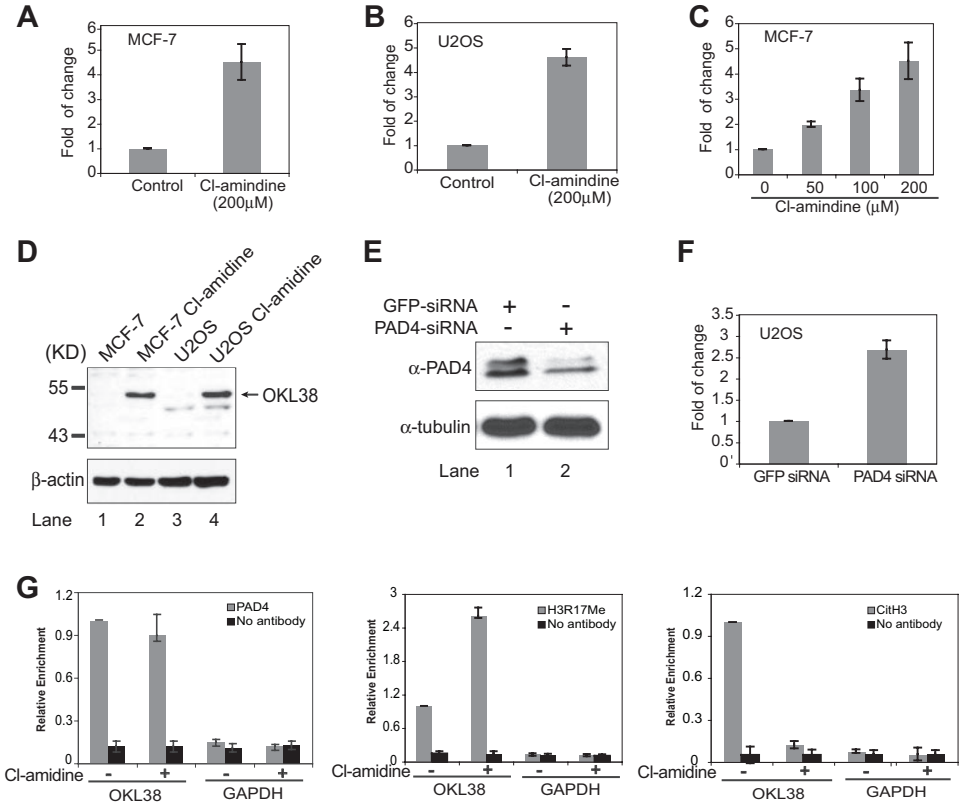

FIGURE 1. **Identification of *OKL38* as a gene regulated by PAD4.** *A* and *B*, effects of Cl-amidine on the expression of *OKL38* in MCF-7 cells (*A*) or U2OS cells (*B*) were analyzed by qRT-PCR at 24 h after Cl-amidine treatment. The amounts of *OKL38* mRNA were normalized with GAPDH. The amount of *OKL38* mRNA without Cl-amidine treatment was normalized as 1-fold. Averages and standard deviations are shown ($n = 3$). *C*, *OKL38* expression was activated by Cl-amidine in a dosage-dependent manner in MCF-7 cells ($n = 3$). *D*, amounts of OKL38 protein were analyzed by Western blot before and after 200 μM Cl-amidine treatment in MCF-7 or U2OS cells. *E*, cells were treated by the PAD4 siRNAs or a control green fluorescent protein siRNA (*GFP-siRNA*) for 3 days. The amounts of PAD4 were analyzed by Western blot. Note the doublet bands of PAD4. *F*, effects of PAD4 depletion on the expression of *OKL38* in U2OS cells were analyzed by qRT-PCR. *G*, PAD4 association, H3R17 methylation, and H3 citrullination levels at the *OKL38* promoter were examined by ChIP in U2OS cells before and after Cl-amidine treatment. Averages of ChIP signals and standard deviations are shown ($n = 3$). Representative PCR results of the ChIP DNA samples are shown in supplemental Fig. S2. The GAPDH promoter was analyzed as a control.

cleotides called BB9, corresponding to the DNA binding consensus sequence specific for human p53 (29), 5′-TGTCCGGGCATGTCCGGGCATGTCCGGGCATGT-3′, the potential p53-binding sites derived from *OKL38* Oligo-1, 5′-GTAGCTGGGATTACAGGTGACCGCCACCATGCCCTGCC-3′, and Oligo-2, 5′-TGCCTGCCCTTAACAGTATCGGCCTTTGTCTTAGTC-3′, were used in these assays. Complementary oligonucleotides were annealed by heat treatment at 95 °C for 5 min and then kept at room temperature for 20 min. Oligonucleotides were end-labeled with [γ-^{32}P]ATP by T4 polynucleotide kinase (New England Biolabs). FLAG-p53 fusion protein was purified from BL21. EMSA was performed in a two-step procedure. In the first step, p53 was activated with monoclonal antibody, PAB421, in the DNA binding buffer (10 mM HEPES, pH 8.0, 50 mM NaCl, 0.1 mM EDTA, 18% glycerol, 0.05% Nonidet P-40, 50 mM dithiothreitol, 4 mM spermidine, 11 μg/ml of poly(dI-dC) for 30 min at room temperature. In the second step, 0.3 ng of labeled DNA probe was added, and a second incubation for 30 min at room temperature was performed. Reaction products were loaded onto a 4% polyacrylamide gel containing TBE. Electrophoresis was performed for 1.5 h at 100 V. Gels were dried and exposed to x-ray film.

Immunostaining and Flow Cytometry Analyses—Immunostaining was performed roughly as described before (15). Living cells were incubated with 150 nM of MitoTracker Red (Invitrogen) for 45 min and then fixed with 4% paraformaldehyde in phosphate-buffered saline for 10 min at room temperature. Samples were washed with PBST and then blocked using PBST containing 2% bovine serum albumin. Anti-FLAG (1:200), anti-OKL38 (1:300), anti-cytochrome *c* (1:200), and anti-NPM (1:500) antibodies were diluted in PBST with 2% bovine serum albumin. Appropriate secondary antibodies, goat anti-mouse fluorescein isothiocyanate (1:200) or Cy3 (1:1000), goat anti-rabbit fluorescein isothiocyanate (1:200), and goat anti-mouse Cy5 (1:1000), were used. After washing three times with PBST, cells were stained with 1 μg/ml Hoechst in PBST. Then the cells were analyzed under the fluorescence microscopy at the Center for Quantitative Cell Analysis at the Pennsylvania State University. To analyze apoptosis, U2OS cells were trypsinized 24 h after the transfection of the FLAG-OKL38 expression plasmid and stained with annexin V (556418, BD Biosciences) and propidium iodide without fixation. Flow cytometry analyses were performed using the FC500 flow cytometer. At least 10, 000 cells were analyzed.

Nuclear Extract Preparations—Procedure is described in detail in the supplemental material.

RESULTS

PAD4 Regulates the Expression of the OKL38 Gene—We and others (13, 15) have previously studied the role of PAD4 in gene regulation using breast cancer MCF-7 cells. To analyze the effects of PAD4 inhibition by Cl-amidine on global gene expression, microarray analyses were performed using MCF-7 cells treated with 200 μM Cl-amidine for 24 h. One of the genes activated by Cl-amidine, pregnancy-induced growth inhibitor/*OKL38/BDGI*, was previously reported to play a role in cell growth inhibition and tumorigenesis (26, 27, 30). To further test the induction of *OKL38* by Cl-amidine, mRNA from MCF-7 cells treated with or without Cl-amidine was analyzed by quantitative reverse transcription-PCR (qRT-PCR). After normalizing mRNA levels to GAPDH, an ~4.5-fold induction of *OKL38* was detected (Fig. 1*A*). Additionally, qRT-PCR assays found that the expression of *OKL38* was induced >4-fold after Cl-amidine treatment in the osteosarcoma U2OS cells (Fig. 1*B*),

suggesting that Cl-amidine can induce *OKL38* expression in multiple cell types. Furthermore, qRT-PCR analyses showed that *OKL38* was activated by Cl-amidine in a dosage-dependent manner (Fig. 1*C*).

To test the change of OKL38 protein levels after Cl-amidine treatment, we generated a rabbit polyclonal antibody against His_6-OKL38 (residues 1–477, NCBI protein accession number AAP14664) expressed in and purified from *Escherichia coli* (supplemental Fig. S1*A*). The antibody was affinity-purified, and the specificity of the antibody was confirmed by antigen competition experiments (supplemental Fig. S1*B*). A band with a molecular mass of ~52 kDa, corresponding to the predicted molecular weight of the 477-amino acid OKL38 protein, was detected after Cl-amidine treatment in MCF-7 and U2OS cells (Fig. 1*D*). In contrast, the amount of OKL38 protein was hardly detectable before Cl-amidine treatment.

As an alternative to PAD4 inhibition by Cl-amidine, we used siRNAs to deplete PAD4 in U2OS cells. The siRNA treatment resulted in >50% decrease in the levels of PAD4 protein (Fig. 1*E*). qRT-PCR assays indicated that the expression of *OKL38* was elevated ~2.5-fold after PAD4 depletion (Fig. 1*F*). These results suggest a repressive role of PAD4 in the expression of *OKL38*.

Because PAD4 can deiminate and demethyliminate histones, we postulated that histone Arg citrullination and methylation might be altered at the *OKL38* promoter after PAD4 inhibition by Cl-amidine. To test this possibility, ChIP assays were performed to analyze PAD4, histone H3 Arg-17 methylation (H3R17Me), and histone H3 citrullination (CitH3) at the *OKL38* promoter in U2OS cells after Cl-amidine treatment. The CitH3 antibody was made against an H3 N-terminal peptide (residues 1–20) containing three citrulline residues (Cit2, -8, and -17) (13). ChIP analyses showed that the amount of PAD4 was not significantly altered at the *OKL38* promoter (Fig. 1*G*). Consistent with PAD4 inhibition by Cl-amidine, histone H3R17Me was increased whereas histone H3 citrullination was decreased at the *OKL38* promoter after Cl-amidine treatment (Fig. 1*G*). As a control, we found that PAD4 did not associate with the GAPDH promoter, and the amount of histone H3 Arg-17 methylation and citrullination was hardly detected (Fig. 1*G*, see also representative gel images in supplemental Fig. S2). These results correlate the decrease of histone citrullination and the increase of histone Arg methylation with the induction of *OKL38* by Cl-amidine.

OKL38 Is a Putative p53 Target Gene—Our results suggest that PAD4 is involved in the regulation of *OKL38*. How PAD4 is targeted to the *OKL38* promoter to regulate transcription is unknown. Because our recent work found that PAD4 interacts with p53 and regulates the expression of the p53 target gene *p21* (17), we postulated that p53 might function as a transcription factor to recruit PAD4 to the *OKL38* promoter. To analyze whether p53 regulates the expression of *OKL38*, the $p53^{-/-}$ lung carcinoma H1299 cells were transiently transfected with a FLAG-p53 expressing plasmid. At 48 h after transfection, a significant increase of *OKL38* mRNA was detected by qRT-PCR (Fig. 2*A*). To further investigate whether the transcriptional activation function of p53 is important for *OKL38* induction, we analyzed the expression of *OKL38* in Tet-On osteosarcoma

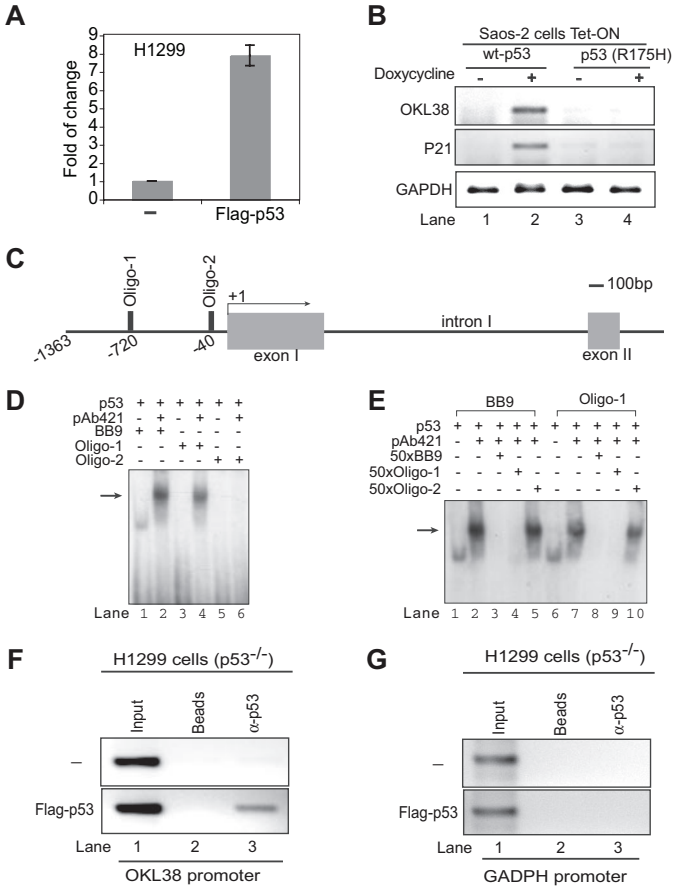

FIGURE 2. **Expression of *OKL38* is regulated by p53.** *A,* change of *OKL38* gene expression was analyzed by qRT-PCR in the $p53^{-/-}$ H1299 cells before and after the expression of p53. OKL38 expression was normalized to GAPDH ($n = 3$). *B,* changes in the *OKL38*, *p21*, and *GAPDH* mRNA levels were monitored by RT-PCR in Tet-On Saos-2 cell lines at 12 h after the addition of doxycycline to induce the expression of wild type p53 or the inactive $p53^{R175H}$ mutant. *C,* schematic drawing of the promoter region of the *OKL38* gene. Exons I and II, intron I, two putative p53-binding sites predicted by the PROMO program were denoted. *D,* p53 bound the positive control BB9 oligo and the Oligo-1 of the *OKL38* promoter, but not Oligo-2, in EMSA. The p53 antibody (PAB421) was used to activate the binding of p53 to its cognate sites in EMSAs. *E,* competition of p53 binding to the radioactive Oligo-1 or BB9 by extra amount of unlabeled BB9, Oligo-1, and Oligo-2. *F,* ChIP assays of the binding of p53 to the *OKL38* promoter in the $p53^{-/-}$ H1299 cells without or with the ectopic expression of FLAG-p53. *G,* as a control, p53 was not associated with the GAPDH promoter without or with the expression of FLAG-p53.

Saos-2 cell lines that express the wild type p53 or an inactive $p53^{R175H}$ mutant that has a defect in activating gene expression (31, 32). Western blot experiments indicated that the wild type p53 and the $p53^{R175H}$ mutant were expressed at comparable levels after treatment with doxycycline for 12 h (supplemental Fig. S3). RT-PCR assays showed that *OKL38* mRNA was increased in Saos-2 cells after the expression of the wild type p53 (Fig. 2*B*, *lanes 1* and *2*), but not in cells after the expression of the $p53^{R175H}$ mutant (Fig. 2*B*, *lanes 3* and *4*), suggesting that the transcriptional activation function of p53 is required for the induction of *OKL38*. In controls, the p53 target gene *p21* was also only induced by the wild type p53, whereas the GAPDH expression was unaltered (Fig. 2*B*). Taken together, the above results suggest that the expression of *OKL38* can be activated by p53.

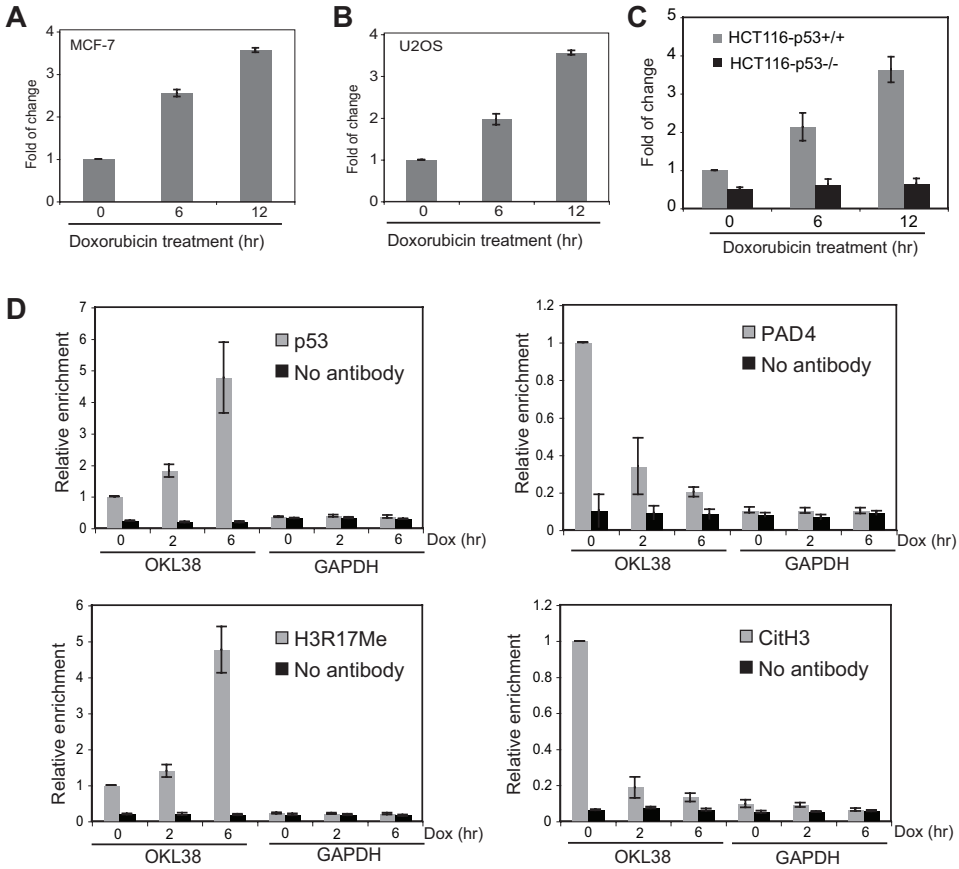

FIGURE 3. ***OKL38* is inducible by DNA damage and its promoter is regulated by dynamic p53 and PAD4 binding and histone Arg modifications.** *A* and *B*, changes of *OKL38* expression detected by qRT-PCR after doxorubicin treatment in MCF-7 cells (*A*) or U2OS cells (*B*). The expression of *OKL38* was normalized with that of GAPDH. *OKL38* expression at 0 h was normalized as 1. Averages and standard deviations are shown ($n = 3$). *C*, levels of the *OKL38* expression were examined by qRT-PCR in the $p53^{+/+}$ and $p53^{-/-}$ HCT116 cells before and after doxorubicin treatment. The expression of *OKL38* in the untreated $p53^{+/+}$ HCT116 cells was normalized as 1. Averages and standard deviations are shown ($n = 3$). *D*, dynamic changes of p53, PAD4, histone H3R17 methylation, and H3 citrullination on the *OKL38* promoter were analyzed by ChIP analyses in MCF-7 cells. Representative PCR results of the ChIP DNA samples are shown in supplemental Fig. S4, *D* and *E*. The amounts of ChIP signals were quantified using the NIH image J program, and signals at 0 h were normalized as 1. Averages and standard deviations are shown ($n = 3$). The GAPDH promoter was analyzed as a control.

We envisioned two scenarios for the activation of *OKL38* by p53, either p53 directly binds to the *OKL38* promoter to activate transcription or p53 indirectly activates *OKL38* via other protein factors. To analyze whether *OKL38* is a downstream target gene of p53, bioinformatics analysis of the *OKL38* promoter was first performed using the PROMO program (supplemental Fig. S4*A*). The PROMO program predicted several putative p53-binding sites in the *OKL38* promoter. Two DNA oligos, Oligo-1 and Oligo-2, containing the predicted p53-binding site at −720 and −40 bp, respectively (Fig. 2*C*, oligo sequences shown in supplemental Fig. S4*B*), were synthesized. The ability of these oligos to bind FLAG-His6-p53 purified from *E. coli* (supplemental Fig. S4*C*) was tested in EMSA. The BB9 oligo, containing a known p53-binding consensus sequence (28), was used as a positive control. Oligo-1 showed p53 binding activity in EMSAs (Fig. 2*D*, *lane 4*) but not Oligo-2 (*lane 6*). Compared with that of BB9 (Fig. 2*D*, *lane 2*), the binding of Oligo-1 to p53 was slightly weaker. To further test the binding specificity, we performed EMSAs with the competition of excessive amounts of unlabeled DNA oligos. As shown in Fig. 2*E*, the binding of p53 to the radioactive BB9 oligo was competed by an excess amount of the unlabeled BB9 oligo (*lane 3*) or Oligo-1 (*lane 4*) but not by Oligo-2 (*lane 5*). Similarly, the binding of the radioactive Oligo-1 to p53 was competed by an excess amount of the unlabeled BB9 (Fig. 2*E*, *lane 8*) or Oligo-1 (*lane 9*) but not by Oligo-2 (*lane 10*). In sum, the −720-bp region of the *OKL38* promoter contains a p53-binding site.

To further analyze whether the −720-bp region of the *OKL38* promoter is associated with p53, ChIP was performed in $p53^{-/-}$ H1299 cells with or without transient transfection of a p53-expressing plasmid. p53 binding to the *OKL38* promoter was detected only after the expression of p53 (Fig. 2*F*, *lane 3, bottom panel*). In control, the GAPDH promoter was not immunoprecipitated by the p53 antibody regardless of the p53 expression status (Fig. 2*G*, *lane 3*). The association of p53 to the *OKL38* was also detected in MCF-7 cells after DNA damage (see Fig. 3).

OKL38 Is Induced by DNA Damage in a p53-dependent Manner and Is Regulated by Histone Arg Modifications—DNA damage activates p53 and induces the expression of p53 target genes (19, 33). To further analyze whether *OKL38* is downstream of the p53 pathway, we treated MCF-7 cells with doxorubicin, a DNA damage-inducing reagent. After normalizing the *OKL38* signals to that of the GAPDH, the expression of *OKL38* was increased ~2.6 and ~3.5-fold at 6 and 12 h after doxorubicin treatment, respectively (Fig. 3*A*), indicating that *OKL38* is induced by DNA damage. An induction of *OKL38* expression was also observed in U2OS cells after doxorubicin treatment (Fig. 3*B*). Next, to analyze whether the induction of *OKL38* by DNA damage is dependent on p53, homotypic $p53^{+/+}$ and $p53^{-/-}$ HCT116 cells were treated with doxorubicin. qRT-PCR analyses showed that *OKL38* expression in $p53^{+/+}$ HCT116 cells was increased ~2- and ~3.6-fold at 6 and 12 h after doxorubicin treatment, respectively (Fig. 3*C*, *gray bars*). In contrast, the levels in *OKL38* expression in $p53^{-/-}$ HCT116 cells remained unaltered after doxorubicin treatment (Fig. 3*C*, *dark bars*), suggesting that *OKL38* is induced by DNA damage in a p53-dependent manner.

Histone Arg methylation has been correlated with the activation of p53 target genes (5), whereas histone deimination and demethylimination catalyzed by PAD4 have been correlated with transcriptional repression (13, 15). To analyze whether histone Arg modifications by PAD4 are involved in the tran-

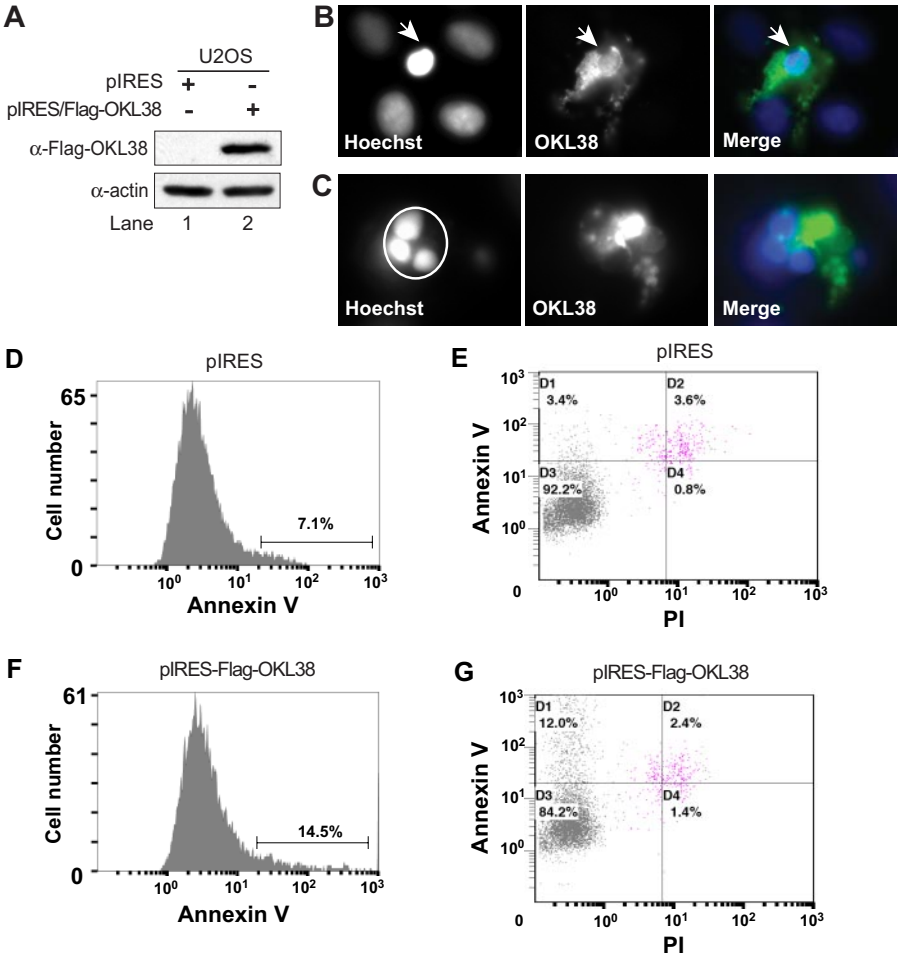

FIGURE 4. **OKL38 overexpression induces apoptosis in U2OS cells.** *A,* FLAG-OKL38 expression was detected at 24 h after transient transfection. Actin was blotted to show equal protein loading. *B,* expression of OKL38 led to the condensation of the nuclear DNA compared with surrounding cells without FLAG-OKL38 expression. *C,* induction of the apoptotic body-like structure formation after the overexpression of FLAG-OKL38. *White circle* outlines a singular nucleus. *D* and *E,* flow cytometry analyses of cells transfected with the pIRES vector and stained with annexin V (*D*) or both annexin V and propidium iodide (*PI*) (*E*). *F* and *G,* flow cytometry analyses of cells transfected with the FLAG-OKL38/pIRES plasmid and stained with annexin V (*F*) or both annexin V and propidium iodide (*G*).

scriptional regulation of *OKL38* during DNA damage, ChIP experiments were performed to analyze p53, PAD4, and histone Arg modifications at the *OKL38* promoter at different time points after doxorubicin treatment in MCF-7 cells. We found that the amount of p53 increased on the *OKL38* promoter at 2- and 6-h time points after doxorubicin treatment (Fig. 3*D*), suggesting that p53 associates with the *OKL38* promoter to regulate transcription after DNA damage. In contrast, the amount of PAD4 detected on the *OKL38* promoter decreased at 2 and 6 h (Fig. 3*D*), suggesting that PAD4 is released from the *OKL38* promoter during transcriptional activation. To test the change of histone Arg modifications at the *OKL38* promoter, we performed ChIP assays with H3 Arg-17 methylation (H3R17Me) and H3 citrullination (CitH3) antibodies. H3R17Me gradually increased on the *OKL38* promoter after DNA damage, suggesting a positive role of histone Arg methylation during the process of *OKL38* induction (Fig. 3*D*). In contrast, the level of CitH3 on the *OKL38* promoter significantly decreased at 2 and 6 h (Fig. 3*D*). This decrease in histone citrullination was correlated with the dissociation of PAD4 from the *OKL38* promoter, which is consistent with the role of PAD4 in histone citrullination. As a control, GAPDH promoter was not associated with p53, PAD4, or dynamic histone Arg modifications after DNA damage. Representative gel images of ChIP assays are shown in supplemental Fig. S4*D*.

OKL38 Overexpression Leads to Apoptosis in U2OS Cells—The expression of OKL38 has been found to be repressed in 60–70% of human kidney and liver cancers (34, 35). Consistent with the idea that the loss of OKL38 expression is beneficial to cancer cell growth (27, 30), we found that the endogenous OKL38 protein in U2OS cells and MCF-7 cells was hard to detect (Fig. 1*D*). To analyze the function of OKL38, we used a plasmid vector to express FLAG-OKL38 in U2OS cells (Fig. 4*A*). FLAG-OKL38 expression in U2OS cells induced nuclear morphology changes characteristic of apoptotic cells (Fig. 4, *B* and *C*). To analyze whether OKL38 overexpression induced phosphatidylserine externalization, a hallmark of apoptosis, we performed annexin V staining in U2OS cells 24 h after transient transfection. In control cells transfected with the pIRES vector alone, 7.1% of U2OS cells were positive for the staining of annexin V (Fig. 4*D*), with 3.4% of cells positive for annexin V only (indication of early apoptotic cells) and 3.6% of cells positive for both annexin V and propidium iodide (measuring cell membrane permeability) staining (Fig. 4*E*). These low percentages of apoptotic cells likely reflect the cytotoxicity of the transfection reagent. In contrast, when the FLAG-*OKL38*/pIRES plasmid was transfected into U2OS cells, the annexin V positive cells were increased to 14.5% (Fig. 4*F*), with 12.0% of cells positive for annexin V and 2.4% of cells positive for both annexin V and propidium iodide (Fig. 4*G*). Because less than 30% of the U2OS cells are routinely transfected in our procedures, the 14.5% of apoptotic cells detected above indicated that a significant percentage of FLAG-OKL38-expressing cells underwent apoptosis.

Translocation of Ectopically Expressed OKL38 to Mitochondria—Although OKL38 overexpression was found to decrease cell growth and increase apoptosis (27, 30), the mechanism by which OKL38 overexpression leads to cell apoptosis is unclear. To address this question, we first analyzed the subcellular distribution of FLAG-OKL38 after ectopic expression in U2OS cells. After transient transfection, FLAG-OKL38 was

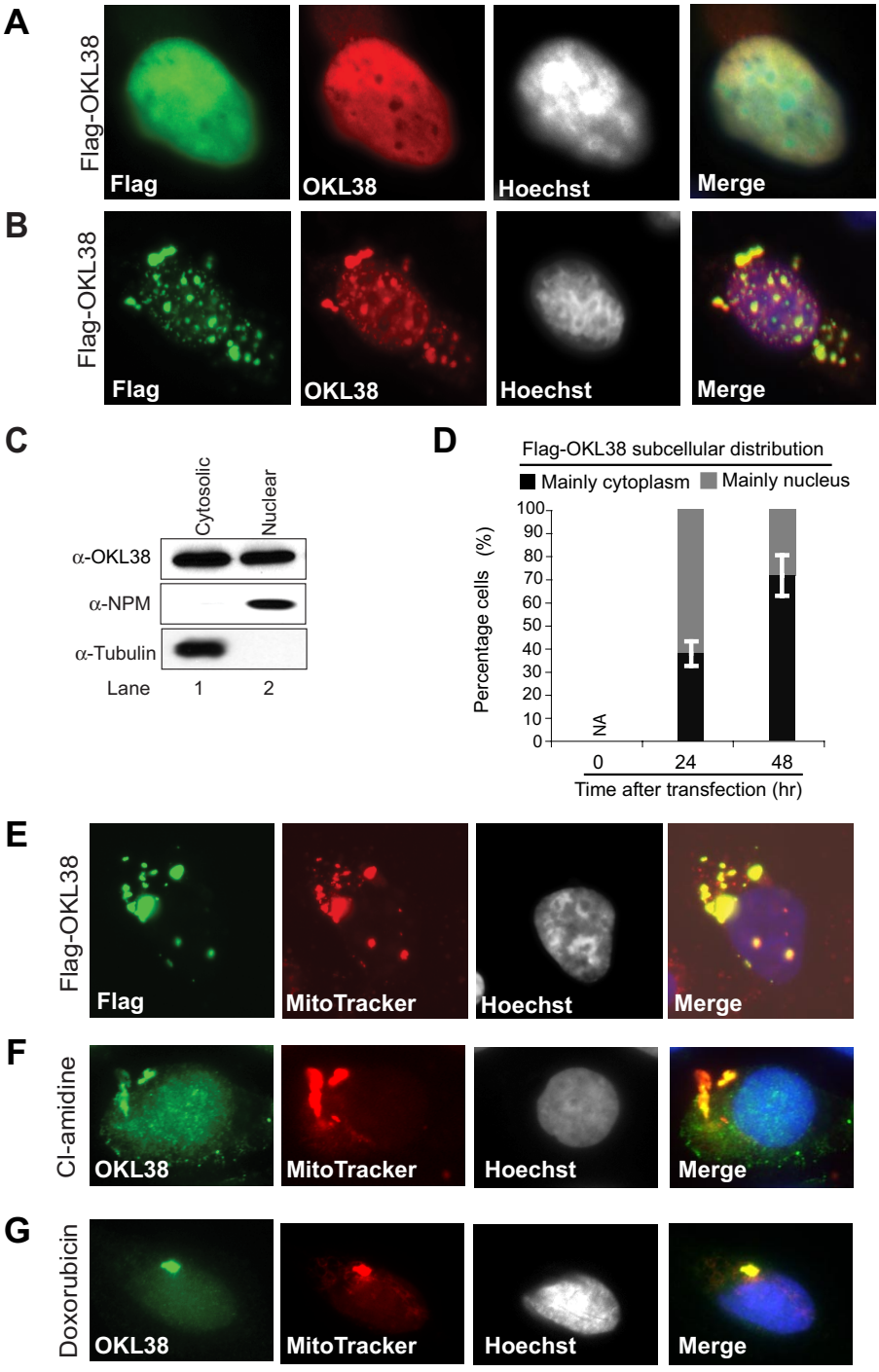

FIGURE 5. **Subcellular localization of OKL38 to nucleus and mitochondria in U2OS cells.** *A,* nuclear localization of FLAG-OKL38 staining was detected in U2OS cells at 24 h after transfection. *B,* spotted cytoplasmic FLAG-OKL38 staining was also detected in U2OS cells at 24 h after transfection. *C,* proteins from U2OS cells expressing FLAG-OKL38 were separated into nuclear and cytoplasmic fractions. The presence of FLAG-OKL38, NPM, and tubulin in the nuclear or cytosolic fractions was analyzed by Western blot. *D,* percentages of cells with mainly cytosolic OKL38 (*dark bars*) or nuclear OKL38 (*gray bars*) were analyzed under the microscope. Over 200 U2OS cells expressing FLAG-OKL38 plasmid were counted at each time points ($n = 3$, standard deviations were shown). *E,* double staining of U2OS cells with the FLAG antibody and a mitochondria dye, MitoTracker, showed the localization of FLAG-OKL38 in mitochondria. *F* and *G,* double staining with the OKL38 antibody and MitoTracker showed that endogenous OKL38 localizes to mitochondria after Cl-amidine (*F*) or doxorubicin (*G*) treatment in U2OS cells.

detected in both nucleoplasm (Fig. 5*A*) and cytoplasm (Fig. 5*B*). To further evaluate the localization of FLAG-OKL38, we generated cytosolic and nuclear fractions from FLAG-OKL38-expressing U2OS cells. Western blot showed that OKL38 was present in both fractions (Fig. 5*C*). As a control for cross-contamination of the two fractions, NPM, a nuclear protein enriched in nucleolus (36), was present only in the nuclear fraction (Fig. 5*C*), whereas tubulin was primarily detected in the cytosolic fraction (Fig. 5*C*), indicating little cross-contamination. Additionally, time course immunostaining analyses found that the percentage of cells with mainly cytoplasmic FLAG-OKL38 staining increased over time (Fig. 5*D*), suggesting that FLAG-OKL38 first accumulated in the nucleus and then became enriched in the cytoplasm.

Intriguingly, FLAG-OKL38 was detected in large speckled structures in U2OS cells (Fig. 5, *B* and *E*). These structures mainly localize to cytoplasm and do not overlap with nucleoli stained by an NPM antibody (supplemental Fig. S5). Such speckled cytoplasmic structures could be mitochondria or lysosomes, which are involved in apoptosis (24) and autophagy (37), respectively. To analyze whether FLAG-OKL38 are localized to these organelles, we performed double staining with the FLAG antibody and the MitoTracker Red dye to stain mitochondria or the cathepsin D antibody to stain lysosomes. We found that FLAG-OKL38 staining in large speckles overlapped with mitochondria (Fig. 5*E*) (over 150 cells scored from three independent experiments). However, OKL38 staining did not colocalize with lysosomes (data not shown).

The inducible expression of *OKL38* by Cl-amidine or doxorubicin prompted us to analyze whether endogenous OKL38 is localized to mitochondria after induction. Immunostaining showed OKL38 localization to mitochondria in U2OS cells after Cl-amidine treatment (Fig. 5*F* and supplemental Fig. S6*A*) or doxorubicin treatment (Fig. 5*G* and supplemental Fig. S6*B*). The localization of endogenous OKL38 to mitochondria was detected in ~7.8% (25/320) and ~13.5% (44/325) of U2OS cells at 24 and 48 h after Cl-amidine treatment, respectively, but not before treatment. Similarly, ~8.4% (18/213) and ~24.7% (65/

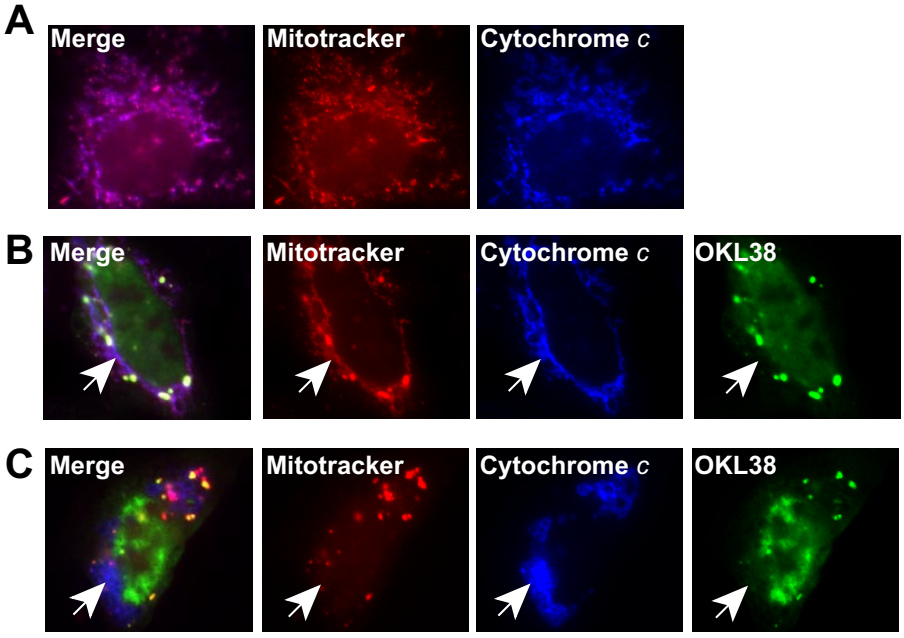

FIGURE 6. **OKL38 overexpression leads to apoptosis, mitochondria structure changes, and the delocalization of cytochrome *c* in U2OS cells.** *A*, in cells without the expression of FLAG-OKL38, the filamentous staining of cytochrome *c* overlapped with the staining of the MitoTracker. The cytochrome *c* staining was pseudocolored *blue*. Mitochondria appear as a continuous network of tubular structures. *B* and *C*, in cells expressing FLAG-OKL38, large and spotted structures were stained by MitoTracker, and the OKL38 antibodies, suggesting a change of mitochondria morphology induced by the OKL38 expression. *White arrows* denote regions with cytochrome *c* staining but lack of MitoTracker staining, indicating the release of cytochrome *c*.

420) of U2OS cells showed mitochondria localization of OKL38 at 24 and 48 h after doxorubicin treatment, respectively. These results indicate that endogenous OKL38 localizes to mitochondria after induction.

Previously, it was found that OKL38 overexpression inhibited cell growth in MCF-7 cells but not in HeLa cells (27). To test whether the mitochondria localization of OKL38 is associated with its proapoptotic function, we analyzed the subcellular localization of OKL38 in HeLa cells. Stable FLAG-OKL38 expression was established in HeLa cells by retrovirus infection (supplemental Fig. S7). OKL38 was detected in the cytoplasm and the nucleus of HeLa cells (supplemental Fig. S7) but not in mitochondria. The lack of mitochondria localization of OKL38 in HeLa cells suggests that mitochondria localization is important for the cell growth inhibition function of OKL38.

OKL38 Overexpression Led to Mitochondrial Morphology Change and Cytochrome c Release—Many apoptosis-inducing signals converge to mitochondria, leading to changes in mitochondria morphology and the release of cytochrome *c* (24, 38, 39). To analyze the effects of FLAG-OKL38 expression on mitochondria morphology and cytochrome *c* localization, we performed triple labeling to detect mitochondria with MitoTracker, cytochrome *c* with a mouse monoclonal antibody, and OKL38 with a rabbit polyclonal antibody in U2OS cells. As shown in Fig. 6*A*, in cells without FLAG-OKL38 expression, filamentous mitochondria structures were stained by both MitoTracker and cytochrome *c*, and overlapping of MitoTracker and cytochrome *c* was observed. After the expression of FLAG-OKL38, a formation of large and spotted mitochondria structures was observed by the MitoTracker staining (Fig. 6, *B* and *C*). Interestingly, overexpression of Bak, a proapoptotic member of the Bcl-2 family of proteins, also caused the formation of speckled mitochondria structures (23). In normally growing cells, cytochrome *c* is localized to mitochondria, whereas the release of cytochrome *c* leads to the activation of caspases and apoptosis (24, 38). In ~19% (32/169) of U2OS cells with speckled OKL38 staining in the cytoplasm, a delocalization of cytochrome *c* from mitochondria was observed (Fig. 6, *B* and *C*, denoted by *arrows*). Taken together, the above results found that OKL38 induced apoptosis in U2OS cells by affecting mitochondria morphology and cytochrome *c* localization.

DISCUSSION

In this study, we showed that 1) the expression of *OKL38* is regulated by p53 and PAD4, and 2) increased OKL38 can induce apoptosis. Our studies suggest that before DNA damage, *OKL38* expression is repressed, and its promoter is associated with low levels of p53 and high levels of PAD4. After DNA damage, PAD4 decreases and p53 increases at the *OKL38* promoter to activate the expression of *OKL38.* Upon elevated expression, OKL38 can translocate to mitochondria leading to the change of mitochondria morphology and apoptosis. We show here that inhibition of the histone-modifying enzyme PAD4 by Cl-amidine activates the expression of tumor suppressor gene *OKL38*. The importance of histone modifications in the control of gene expression during normal and cancerous cell growth has been recognized in recent years (40–42). A paradigm of epigenetic histone modifications in tumorigenesis is emerging, *i.e.* epigenetic silencing of tumor suppressor genes or activation of oncogenes mediated by histone modifications and DNA methylation participates in the early stage of tumorigenesis.

We have previously shown that PAD4 represses gene expression by regulating Arg methylation and citrullination in histones (15). PAD4 regulates gene expression by counteracting the functions of protein Arg methyltransferases via two possible mechanisms, by deimination to prevent subsequent Arg methylation or by demethylimination to decrease the level of histone Arg methylation (13). Here we show that after inhibition of PAD4 by Cl-amidine to activate *OKL38* expression, histone Arg methylation increased whereas histone citrullination decreased at the *OKL38* promoter. Additionally, upon DNA damage to activate the expression of *OKL38*, PAD4 association and histone citrullination at the

OKL38 promoter was decreased with a concomitant increase in histone Arg methylation at the *OKL38* promoter. These results suggest that histone Arg modifications play a dynamic role in the regulation of *OKL38*. We also found that *OKL38* is a p53 target gene that is inducible by DNA damage. The expression of wild type p53 but not the $p53^{R175H}$ mutant was sufficient to induce the expression of *OKL38*. A p53-binding site in the *OKL38* promoter was identified by both EMSA and ChIP experiments. The DNA damage reagent doxorubicin increased *OKL38* expression in a p53-dependent manner in the $p53^{+/+}$ but not $p53^{-/-}$ colon cancer HCT116 cells. Furthermore, upon *OKL38* activation by doxorubicin, the levels of p53 were increased at the *OKL38* promoter, suggesting that p53 plays a positive role in the activation of *OKL38* after DNA damage. A recent study has shown that the expression of *OKL38* is induced by oxidative stress (43), suggesting that *OKL38* can be regulated by multiple extracellular signals.

OKL38 also seems to play an important role in apoptosis. Previous studies have found that the overexpression of OKL38 induced cell death in A498 (kidney cancer), buffalo rat liver, and MCF-7 (breast cancer) cells (27, 34, 35). However, the mechanisms by which OKL38 overexpression induced apoptosis remained unclear. We found that the translocation of OKL38 to mitochondria eventually led to mitochondria morphology changes, cytochrome *c* release, and cell death in U2OS cells. Interestingly, upon overexpression, OKL38 was not targeted to mitochondria in HeLa cells and did not induce cell growth inhibition or cell death. Thus, our studies of the mitochondria localization of OKL38 may offer a molecular mechanism by which OKL38 induces cell death.

The role of p53 in gene regulation has been extensively studied. Following activation, p53 turns on the expression of a class of proapoptotic genes, such as *BAX*, *NOXA*, and *PUMA*, which encode effector proteins that regulate the permeability of mitochondria outer membrane and induce cytochrome *c* release (18, 19). Because OKL38 induces apoptosis and localizes to mitochondria and regulates cytochrome *c* release, OKL38 likely belongs to the proapoptotic class of the p53 target genes. The expression of *OKL38* is normally induced during pregnancy and lactation in the rat mammary gland, which was proposed to contribute to the cell growth arrest and terminal cell differentiation (30). The loss or decrease of OKL38 protein has been reported in over 60% of hepatocellular carcinoma (26), suggesting that OKL38 may function as a tumor suppressor. How cancer cells gained growth advantage after the loss of OKL38 expression as well as how OKL38 induces cytochrome *c* release await future investigation.

Acknowledgments—We thank Drs. Y. Dou (University of Michigan), X. Zhang (University of Cincinnati), Y. Tian (University of Texas A & M), K. M. Ryan (Beatson Institute for Cancer Research, UK), B. Vogelstein (The Johns Hopkins University), and H. Wang (University of Alabama) for plasmids and cell lines. We thank Drs. D. Gilmour, J. Reese, and S. Tan for helpful discussions and Dr. R. Schlegel for critical reading of the manuscript.

REFERENCES

1. Shilatifard, A. (2006) *Annu. Rev. Biochem.* **75,** 243–269
2. Strahl, B. D., and Allis, C. D. (2000) *Nature* **403,** 41–45
3. Li, B., Carey, M., and Workman, J. L. (2007) *Cell* **128,** 707–719
4. Huang, S., Litt, M., and Felsenfeld, G. (2005) *Genes Dev.* **19,** 1885–1893
5. An, W., Kim, J., and Roeder, R. G. (2004) *Cell* **117,** 735–748
6. Bauer, U. M., Daujat, S., Nielsen, S. J., Nightingale, K., and Kouzarides, T. (2002) *EMBO Rep.* **3,** 39–44
7. Bedford, M. T., and Richard, S. (2005) *Mol. Cell* **18,** 263–272
8. Chen, D., Ma, H., Hong, H., Koh, S. S., Huang, S. M., Schurter, B. T., Aswad, D. W., and Stallcup, M. R. (1999) *Science* **284,** 2174–2177
9. Wang, H., Huang, Z. Q., Xia, L., Feng, Q., Erdjument-Bromage, H., Strahl, B. D., Briggs, S. D., Allis, C. D., Wong, J., Tempst, P., and Zhang, Y. (2001) *Science* **293,** 853–857
10. Hagiwara, T., Nakashima, K., Hirano, H., Senshu, T., and Yamada, M. (2002) *Biochem. Biophys. Res. Commun.* **290,** 979–983
11. Nakashima, K., Hagiwara, T., and Yamada, M. (2002) *J. Biol. Chem.* **277,** 49562–49568
12. Vossenaar, E. R., Zendman, A. J., van Venrooij, W. J., and Pruijn, G. J. (2003) *BioEssays* **25,** 1106–1118
13. Cuthbert, G. L., Daujat, S., Snowden, A. W., Erdjument-Bromage, H., Hagiwara, T., Yamada, M., Schneider, R., Gregory, P. D., Tempst, P., Bannister, A. J., and Kouzarides, T. (2004) *Cell* **118,** 545–553
14. Klose, R. J., and Zhang, Y. (2007) *Nat. Rev. Mol. Cell Biol.* **8,** 307–318
15. Wang, Y., Wysocka, J., Sayegh, J., Lee, Y. H., Perlin, J. R., Leonelli, L., Sonbuchner, L. S., McDonald, C. H., Cook, R. G., Dou, Y., Roeder, R. G., Clarke, S., Stallcup, M. R., Allis, C. D., and Coonrod, S. A. (2004) *Science* **306,** 279–283
16. Balint, B. L., Szanto, A., Madi, A., Bauer, U. M., Gabor, P., Benko, S., Puskas, L. G., Davies, P. J., and Nagy, L. (2005) *Mol. Cell. Biol.* **25,** 5648–5663
17. Li, P., Yao, H., Zhang, Z., Li, M., Luo, Y., Thompson, P. R., Gilmour, D. S., and Wang, Y. (2008) *Mol. Cell Biol.*, in press
18. Harris, S. L., and Levine, A. J. (2005) *Oncogene* **24,** 2899–2908
19. Vogelstein, B., Lane, D., and Levine, A. J. (2000) *Nature* **408,** 307–310
20. Selvakumaran, M., Lin, H. K., Miyashita, T., Wang, H. G., Krajewski, S., Reed, J. C., Hoffman, B., and Liebermann, D. (1994) *Oncogene* **9,** 1791–1798
21. Oda, K., Arakawa, H., Tanaka, T., Matsuda, K., Tanikawa, C., Mori, T., Nishimori, H., Tamai, K., Tokino, T., Nakamura, Y., and Taya, Y. (2000) *Cell* **102,** 849–862
22. Oda, E., Ohki, R., Murasawa, H., Nemoto, J., Shibue, T., Yamashita, T., Tokino, T., Taniguchi, T., and Tanaka, N. (2000) *Science* **288,** 1053–1058
23. Brooks, C., Wei, Q., Feng, L., Dong, G., Tao, Y., Mei, L., Xie, Z. J., and Dong, Z. (2007) *Proc. Natl. Acad. Sci. U. S. A.* **104,** 11649–11654
24. Jiang, X., and Wang, X. (2004) *Annu. Rev. Biochem.* **73,** 87–106
25. Luo, Y., Arita, K., Bhatia, M., Knuckley, B., Lee, Y. H., Stallcup, M. R., Sato, M., and Thompson, P. R. (2006) *Biochemistry* **45,** 11727–11736
26. Ong, C. K., Leong, C., Tan, P. H., Van, T., and Huynh, H. (2007) *Oncogene* **26,** 1155–1165
27. Wang, T., Xia, D., Li, N., Wang, C., Chen, T., Wan, T., Chen, G., and Cao, X. (2005) *J. Biol. Chem.* **280,** 4374–4382
28. Bensaad, K., Tsuruta, A., Selak, M. A., Vidal, M. N., Nakano, K., Bartrons, R., Gottlieb, E., and Vousden, K. H. (2006) *Cell* **126,** 107–120
29. Halazonetis, T. D., and Kandil, A. N. (1993) *EMBO J.* **12,** 5057–5064
30. Huynh, H., Ng, C. Y., Ong, C. K., Lim, K. B., and Chan, T. W. (2001) *Endocrinology* **142,** 3607–3615
31. Crighton, D., Wilkinson, S., O'Prey, J., Syed, N., Smith, P., Harrison, P. R., Gasco, M., Garrone, O., Crook, T., and Ryan, K. M. (2006) *Cell* **126,** 121–134
32. Ryan, K. M., Ernst, M. K., Rice, N. R., and Vousden, K. H. (2000) *Nature* **404,** 892–897
33. Laptenko, O., and Prives, C. (2006) *Cell Death Differ.* **13,** 951–961
34. Ong, C. K., Ng, C. Y., Leong, C., Ng, C. P., Foo, K. T., Tan, P. H., and Huynh, H. (2004) *J. Biol. Chem.* **279,** 743–754
35. Ong, C. K., Ng, C. Y., Leong, C., Ng, C. P., Ong, C. S., Nguyen, T. T., and

Huynh, H. (2004) *Endocrinology* **145,** 4763–4774
36. Okada, M., Jang, S. W., and Ye, K. (2007) *J. Biol. Chem.* **282,** 36744–36754
37. Baehrecke, E. H. (2005) *Nat. Rev. Mol. Cell Biol.* **6,** 505–510
38. Cereghetti, G. M., and Scorrano, L. (2006) *Oncogene* **25,** 4717–4724
39. Youle, R. J., and Karbowski, M. (2005) *Nat. Rev. Mol. Cell Biol.* **6,** 657–663
40. Esteller, M. (2007) *Br. J. Cancer* **96,** (suppl.) R26–R30
41. Marks, P. A., and Breslow, R. (2007) *Nat. Biotechnol.* **25,** 84–90
42. Mund, C., Brueckner, B., and Lyko, F. (2006) *Epigenetics* **1,** 7–13
43. Li, R., Chen, W., Yanes, R., Lee, S., and Berliner, J. A. (2007) *J. Lipid Res.* **48,** 709–715